Pergamon

PII: S0079-1946(98)00080-9

Phys. Chem. Earth, Vol. 23, No. 5–6, pp. 599–604, 1998

0079-1946/98/$ - see front matter

Simulated Long-wave Clear-sky Irradiance over the Ocean: Spatial and Temporal Variability 1979–1993

R. P. Allan[1] and A. Slingo[2]

[1]Department of Meteorology, University of Reading, Reading, RG6 6BB, United Kingdom
[2]Hadley Centre, Meteorological Office, London Road, Bracknell, RG12 2SY, United Kingdom

Received 25 April 1997; accepted 22 September 1997

Abstract. Clear-sky long-wave irradiances calculated by a wide-band radiation code applied to the ECMWF re-analysis are used to investigate the spatial and temporal variations in net surface long-wave radiative fluxes over the ocean. Monthly mean clear-sky net long-wave irradiances from the atmosphere to the ocean surface, F_{net} (Wm^{-2}), are presented for the period 1979 to 1993. F_{net} is of order -90 Wm^{-2} between sea surface temperatures (T_s) of 270 and 295 K. For T_s greater than 295 K there is an increase in F_{net} to approximately -60 Wm^{-2} at 300 K. This feature is present throughout the year. The average dF_{net}/dT_s in the seasonal cycle (July-January) for 1985 is 5.3 $Wm^{-2}K^{-1}$. Irradiance variation on daily to decadal time-scales are considered. Comparisons with observations in the tropical West Pacific and with a simple expression developed by Prata (Quart. J. Roy. Met. Soc., 1996) are undertaken. Increases in surface emission are generally offset by increases in the downwelling component of F_{net} on all time-scales considered; this may be explained by simple thermodynamics. Large perturbations to atmospheric temperature and moisture over the seasonal cycle are required to explain spatially widespread positive dF_{net}/dT_s.

1 Introduction

The clear-sky net long-wave irradiance at the surface (here defined as downwelling minus upwelling irradiance), F_{net} (Wm^{-2}), constitutes a significant component of the surface energy budget. It also plays a fundamental role in the potential positive water vapour feedback to surface warming (IPCC, 1990). Seager et al. (1995) note that variations in F_{net} contribute markedly to the variation of heat flux into the ocean which is particularly relevant for sophisticated coupled atmosphere-ocean models. Therefore validation and simulation of the clear-sky long-wave irradiance at the surface is important in climate studies. The effects of clouds are not considered in this study which aims to provide information concerning the water vapour feedback to sea surface temperatures.

This study sets out to characterise the global variation of F_{net} over the ocean (Sect. 3) using the models and data described in Sect. 2. The variation of F_{net} over seasonal to decadal time-scales is assessed in Sect. 4. Comparison with a simple expression developed by Prata (1996) in Sect. 5 and with observations in the tropical West Pacific (Weller and Anderson, 1996) are undertaken which constitutes an attempt at validating simulated irradiances (Sect. 6). Conclusions are drawn in Sect. 7.

2 Simulation description

The clear-sky long-wave (0-3000 cm^{-1}) net irradiance at the ocean surface is calculated by a wide-band version of the Edwards and Slingo (1996) radiation scheme which is applied to the European Centre for Medium range Weather Forecasts (ECMWF) re-analysed atmospheric profiles of temperature and water vapour. The simulation, hereafter referred to as CLERA, is described in detail in Slingo et al. (1997). Emission by water vapour, carbon dioxide, ozone, methane, nitrous oxide, CFC11 and CFC12 were accounted for and the surface is assumed to emit as a black body. Calculations were performed every 6 hours from 1979 to 1993 inclusive over a 2.5 by 2.5 degree grid. Sea surface temperatures are based on Reynolds (1988).

3 Global irradiance variability

F_{net} is least negative in tropical oceans and most negative in the northern hemisphere winter, especially at

Correspondence to: R. P. Allan

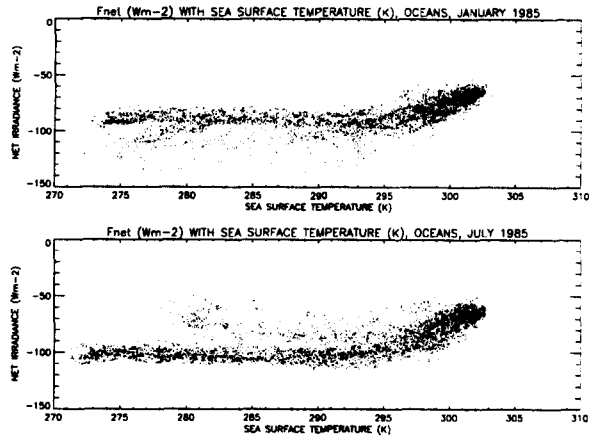

Fig. 1. F_{net} (Wm^{-2}) plotted with sea surface temperatures (K) over the oceans for January (top) and July (bottom) 1985 between 60°S and 60°N.

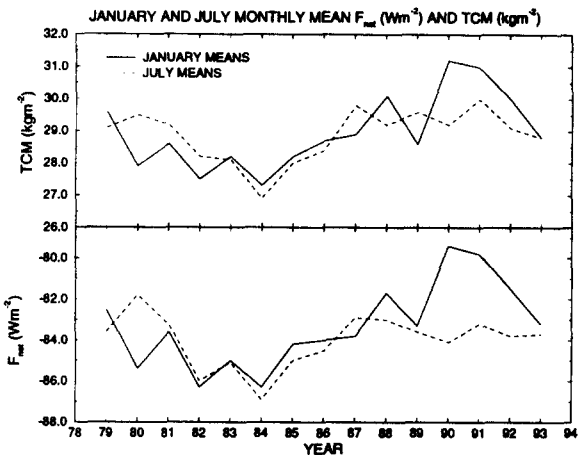

Fig. 2. Decadal variation of total column moisture, u (kgm^{-2}) (top) and F_{net} (Wm^{-2}) (bottom) for January and July means over the oceans between 60°S and 60°N.

high latitudes over the warm sea surfaces on the western side of the ocean basins. Figure 1 shows F_{net} in 1985 to remain of order -90 to -100 Wm^{-2} between sea surface temperatures (T_s) of 270 and 295 K. This shows that atmospheric emission of clear-sky long-wave irradiance changes at approximately the same rate as surface upwelling emission between these temperatures. Above about 295 K there is a tendency for F_{net} to increase (become less negative) with increasing T_s. Therefore downwelling long-wave irradiance at the surface is increasing at a greater rate than surface upwelling emission with sea surface temperature; this is consistent with the surface super greenhouse effect as defined by Vonder Haar (1986) and may be explained by the large increases in total column moisture with increasing surface temperatures in tropical regions. The general pattern in Fig. 1 applies to monthly means throughout the simulation period.

The mean F_{net} over the oceans between 60°S and 60°N is -84.2 Wm^{-2} in January and -84.9 Wm^{-2} in July. The northern hemisphere F_{net} varies between July and January more than southern hemisphere F_{net}. This is because the greater land area in the northern hemisphere causes large perturbations to atmospheric structure over the annual cycle. Therefore downwelling long-wave irradiance at the surface varies to a much greater extent between summer and winter than in the southern hemisphere. This is discussed further in the context of the atmospheric greenhouse effect by Webb et al. (1993).

4 Temporal variability

Temporal changes in F_{net} with T_s may be characterised by

$$\frac{dF_{net}}{dT_s} = \frac{\partial F_{net}}{\partial u}\frac{\partial u}{\partial T_s} + \frac{\partial F_{net}}{\partial T(p)}\frac{\partial T(p)}{\partial T_s} - 4\sigma T_s^3, \qquad (1)$$

where $T(p)$ denotes the atmospheric temperature structure as a function of pressure, p. The Stefan-Boltzmann constant, $\sigma = 5.67\text{x}10^{-8}\ Wm^{-2}K^{-4}$ and u is the total column moisture (kgm^{-2}). The first two terms of the right hand side of Eq. (1) denote the changes in irradiance due to changes in column moisture and atmospheric temperature respectively, while the final term denotes the change in surface emission with surface temperature. Using a 10 cm^{-1} resolution long-wave radiation code resolved between 0 and 3000 cm^{-1} (Shine (1991)) and a tropical standard atmosphere (McClatchey et al. (1972)), the sensitivity of F_{net} to idealised temperature and water vapour perturbations is assessed. For pressures greater than 400 mb, temperature change is prescribed by,

$$\frac{dT(p)}{dT_s} = \frac{p - 400}{p_s - 400}, \qquad (2)$$

where p is atmospheric pressure (mb) and p_s is surface pressure (mb). For pressures less than or equal to 400 mb, temperature remains constant. This temperature change is chosen to be loosely consistent with lower tropospheric warming observed by Angell (1988). Water vapour mass mixing ratio is increased so as to hold relative humidity constant, akin to the study by Manabe and Wetherald (1967). The resulting dF_{net}/dT_s of 2.5 $Wm^{-2}K^{-1}$ for a 1 K increase in T_s is comprised of 4.4 $Wm^{-2}K^{-1}$ due to atmospheric temperature changes, 4.2 $Wm^{-2}K^{-1}$ due to atmospheric column moisture changes and -6.1 $Wm^{-2}K^{-1}$ due to surface emission changes. This shows that for this particular tropospheric warming scenario, changes in atmospheric temperature and water vapour contribute approximately equally to increasing F_{net} for the tropical profile. The decrease in F_{net} due to surface emission decreases is overwhelmed by increases in downwelling long-wave emission, thus introducing a thermodynamically driven surface super-greenhouse effect.

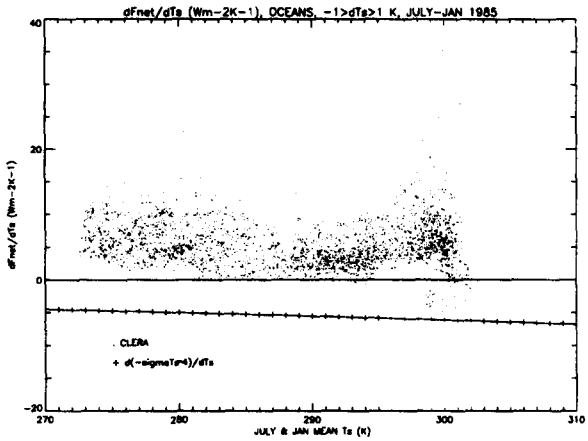

Fig. 3. dF_{net}/dT_s $(Wm^{-2}K^{-1})$ over the seasonal cycle (July minus January, 1985) with mean T_s. Ocean grid points between 60 °S and 60 °N for temperature changes greater than 1 K are plotted.

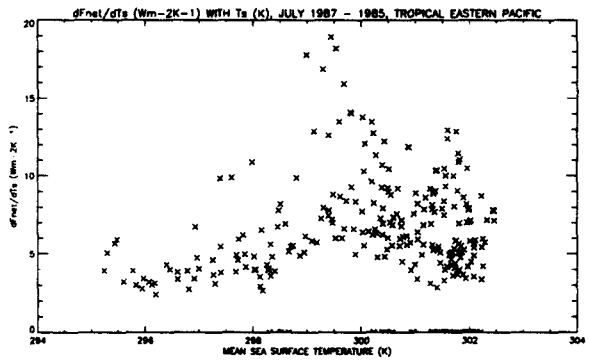

Fig. 4. Interannual (Change in F_{net})/(Change in T_s) $(Wm^{-2}K^{-1})$ for July in the Tropical East Pacific, 1987 minus 1985, plotted with T_s (K). -1> dT_s >1 K.

Figure 2 shows the January and July monthly mean F_{net} between 60 °S and 60 °N to vary by over 5 Wm^{-2} (about 6 %) over the decadal time scale. This variation is closely correlated with variations in total column moisture, u (kgm^{-2}). Using linear regression, dF_{net}/du is calculated to be 1.7 Wkg^{-1} with a correlation coefficient of 0.95. Changes in total column moisture dominate over changes in atmospheric temperature in determining the F_{net} variation over a decadal time-scale because mean near-surface temperature varies little (less than 0.4 K).

Over the seasonal cycle (July minus January) changes in F_{net} at a particular location are large (of order tens of Wm^{-2}) in all but the lower latitudes. The 60 °S to 60 °N area mean (over the oceans) dF_{net}/dT_s over the seasonal cycle is 5.3 $Wm^{-2}K^{-1}$ which constitutes a strong, positive clear-sky long-wave radiative feedback to surface temperatures. Figure 3 shows dF_{net}/dT_s for each grid point where the magnitude of temperature changes are greater than 1 K. All but two grid points are above the line, $dF_{net}/dT_s = -4\sigma T_s^3$ which marks the change in F_{net} with T_s if there is no change in surface downwelling long-wave irradiance (crossed line in fig. 2). Thus atmospheric long-wave downwelling emission from the atmosphere to the ocean surface acts to offset significantly the surface upwelling emission changes over the seasonal cycle.

dF_{net}/dT_s is large at high latitudes because the change in atmospheric profile over the seasonal cycle is large for the given change in T_s. High values of dF_{net}/dT_s at low latitudes are explained by the large change in column moisture for a given change in surface temperature which is a result of the Clausius-Clapeyron relationship (e.g., Hess, 1959) and the coupling between atmospheric and surface temperatures. The largest values of dF_{net}/dT_s (as much as 35 $Wm^{-2}K^{-1}$) are experienced in the coastal regions of India, and are a likely consequence of the large perturbations to atmospheric structure over the monsoon cycle.

Interannual variability of F_{net} is less correlated with T_s variability due to the lower perturbations to surface temperatures and atmospheric profiles. However, large changes in surface temperatures associated with large-scale perturbations to atmospheric profiles during El-Niño and La-Niña years results in large positive values of dF_{net}/dT_s. Figure 4 shows dF_{net}/dT_s for grid points between 10 °S and 10 °N, 180 to 270 °E for 1987 minus 1985 in July. dF_{net}/dT_s is greater than zero for all grid points and the mean value is 7.4 $Wm^{-2}K^{-1}$. Area mean dF_{net}/dT_s between months (i.e. July minus June) is generally positive, although there is a spread of most values between ± 20 $Wm^{-2}K^{-1}$.

5 Comparison with a simple formula

Using a simple formula to estimate F_{net} acts as an independent test for the CLERA simulation. While errors in both methods discount the possibility of irradiance validation, biases in the simulation may be highlighted. Using ECMWF values of near-surface temperature, T_0 (K), and near-surface water vapour pressure, e_0 (Pa), an expression developed by Prata (1996) is used to estimate surface net clear-sky long-wave irradiance (Wm^{-2}):

$$F_{prata} = \sigma T_0^4[1 - (1 + \frac{u}{10})exp-(1.2 + \frac{3u}{10})^{\frac{1}{2}}] - \sigma T_s^4, \quad (3)$$

$$u = C\frac{e_0}{T_0}. \quad (4)$$

The relationship in Eq. (4) is empirically determined from observations with a best fit at C= 4.65 Ks^2m^{-1} (Prata (1996)), while Eq. (3) is based on radiative transfer theory, and so acts as a framework to assess the performance of the CLERA simulation.

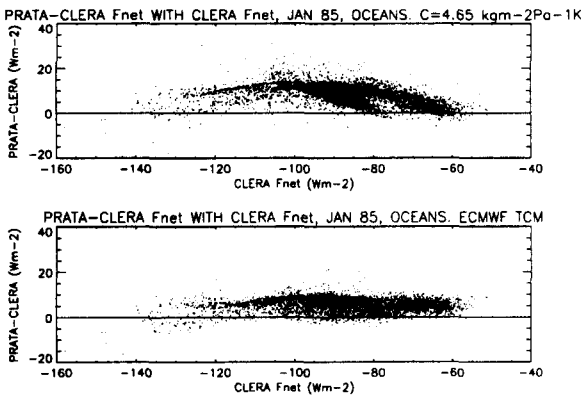

Fig. 5. $F_{prata} - F_{net}$ (Wm^{-2}) plotted against F_{net} (Wm^{-2}) for $C = 4.65\ Ks^2m^{-1}$ (top) and ECMWF u (bottom) for January 1985.

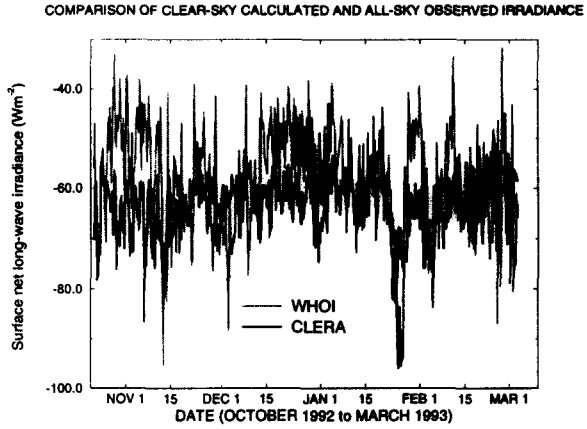

Fig. 6. Six hourly F_{net} (Wm^{-2}) and filtered six hourly F_{whoi} (Wm^{-2}) from 21 October 1992 to 4 March 1993 in the tropical Western Pacific.

Figure 5 shows $F_{prata} - F_{net}$ plotted against F_{net} for C= 4.65 Ks^2m^{-1} (top) and also using the ECMWF values of u (bottom) for January 1985 means. The scatter in $F_{prata} - F_{net}$ over the oceans, globally, of about 20 Wm^{-2} is small considering the simplicity of the formula and the accuracy of radiative transfer schemes and in situ observations. Mean F_{prata} minus F_{net} equals 7.7 Wm^{-2} when C equals 4.65 Ks^2m^{-1}. Middle latitude differences tend to be positive, while differences are small in low and high latitudes. $F_{prata} - F_{net}$ equals 1.7 Wm^{-2} when C is 4.0 Ks^2m^{-1} (not shown). This implies that the water vapour scale height implicitly accounted for in the parameter, C, is of a greater magnitude than the mean ECMWF value. When u derived from ECMWF data is used in Eq. 2, $F_{prata} - F_{net}$ values lie mostly between 0 and 10 Wm^{-2} with a mean difference of 5.4 Wm^{-2}. Using ECMWF u rather than using Eq. 4 decreases the spread of values. This indicates a modest failure in Eq. 4 in estimating u, globally, from surface screen conditions. The systematic positive difference suggests that either F_{prata} values are too high or F_{net} values are too negative, or both. Indeed, global mean CLERA F_{net} are less than values derived by Rossow and Zhang (1995) as discussed in Slingo et al. (1997). One source of this discrepancy could be that ECMWF profiles are too dry.

6 Comparison with in situ obsevations

All-sky (i.e. clear and overcast sky) surface net long-wave irradiance measured by the Woods Hole Oceanographic Institute buoy (F_{whoi}) (Weller and Anderson, 1996) are compared with 6-hourly values of F_{net} over the period 21 October 1992 to 4 March 1993. F_{whoi} was measured in the tropical Western Pacific at 156 °E, 2.5 °S; the nearest CLERA grid point was taken as 155 °E, 2.5 °S. Figure 6 shows the F_{net} and 6-hour filtered F_{whoi} comparison.

The mean F_{whoi} of -58.1 Wm^{-2} is less negative than the mean F_{net} of -63.2 Wm^{-2}. This is in part due to clouds in the observations acting to make the net long-wave irradiance less negative, but also due to simulation and observation errors. The presence of clouds in the observations and the more averaged nature of CLERA atmospheric profiles causes F_{whoi} variation (standard deviation of 10.4 Wm^{-2}) to be greater than F_{net} variation (standard deviation of 6.9 Wm^{-2}) over the six-hourly time-scale. It should be noted that the F_{net} variability is determined primarily by variations in the surface downwelling long-wave irradiance due to small variations in surface emission over a daily time-scale. F_{whoi} variability is determined also by a significant observed diurnal variation of surface long-wave emission.

The direct comparison suggests F_{net} is not negative enough or that the observations are too negative, or both. This is concluded because the all-sky observations should intuitively be greater than the clear-sky simulation because clouds act to increase the net surface downwelling irradiance. However F_{net} is shown to be greater than observed irradiance over periods of days (i.e. early December, Fig. 6). Work by Dutton (1993) also reproduces this calculation minus observation positive difference.

Figure 6 also shows time-periods when both F_{net} and F_{whoi} are very negative (less than -80 Wm^{-2}), most notably centred on 14 November and 25 January. A time-latitude plot between 17.5 and -20 °N in November of F_{net} anomalies from the monthly mean shows the very negative values to propagate from the south (Fig. 7). This is due to a tongue of relatively dry air moving northwards from Australia which coincides with the transition between phases of the Intraseasonal Oscillation (ISO) as discussed by Gutzler et al. (1994).

To assess potential simulation errors due to ECMWF

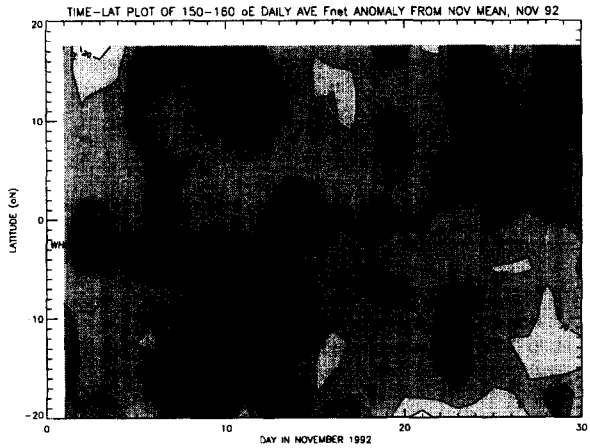

Fig. 7. Time-latitude plot between 17.5 and -20 °N of F_{net} (Wm^{-2}), anomalies from the November 1992 mean. Contour interval, 10 Wm^{-2}.

profile disparities, radiosonde retrievals from Kavieng (150.8 °E, 2.6 °S) (Long (1995)) are utilised in conjunction with corresponding ECMWF profiles. The Shine (1991) radiation code is used to calculate clear-sky surface downwelling long-wave irradiances (Table 1). The profiles considered are chosen to sample relatively dry ($u < 50\ kgm^{-2}$) and relatively moist ($u > 50\ kgm^{-2}$) conditions for a range of times. The ECMWF profile mean u is 3.9 % greater than radiosonde profile mean u (which is inconsistent with the hypothesis that ECMWF profiles are too dry). This corresponds with mean calculated irradiance for the ECMWF profiles being 4.8 Wm^{-2} greater than mean calculated irradiance for the radiosonde profiles. However, it is shown by replacing radiosonde surface temperatures with ECMWF values (radiosonde′ in Table 1) that much of the disparity in calculated irradiance is attributable to surface temperature differences rather than total column moisture differences. Root mean squared ECMWF minus radiosonde irradiance differences of 8.2 Wm^{-2} decrease to 1.8 Wm^{-2} for ECMWF minus radiosonde′ values. This highlights the importance of near-surface layer temperature in determining surface downwelling long-wave irradiance as discussed by Zhao et al. (1994). Therefore specification of surface temperature and interpolation of near-surface temperature is likely to significantly influence simulation accuracy for F_{net}. CLERA near-surface temperature and T_s are essentially coupled (Edwards (1997) pers. com) which is in contradiction with observations (Weller and Anderson, 1996), thus introducing a bias into the simulated F_{net}.

Table 1. Calculated surface downwelling long-wave irradiance for ECMWF, radiosonde profiles, and radiosonde profiles with ECMWF surface temperature (radiosonde′) at 150.8 °E, 2.6 °S

Date, Time (GMT)	ECMWF (Wm^{-2})	Radiosonde (Wm^{-2})	Radiosonde′ (Wm^{-2})
11/11/92, 12z	418.9	406.4	415.2
13/11/92, 12z	407.5	397.3	408.6
29/12/92, 00z	415.9	404.5	415.3
31/12/92, 00z	403.2	405.9	403.5
23/1/93, 06z	419.9	421.6	421.6
24/1/93, 06z	405.5	406.2	404.1
Mean:	411.8	407.0	411.4

7 Conclusion

Simulated clear-sky long-wave net irradiances at the surface over the ocean are presented for the period 1979 to 1993. The mean F_{net} between 60 °S and 60 °N varies by about 5 Wm^{-2} for July means and about 7 Wm^{-2} for January means over the entire period. The simulated variation is explained primarily by changes in total column moisture as there is only small interannual variability in mean monthly T_s.

At surface temperatures below about 295 K F_{net} is of order -90 Wm^{-2} and spatial variability is low. Increases in atmospheric temperature and total column moisture with increasing surface temperature cause surface downwelling long-wave emission to increase at approximately the same rate as surface upwelling emission with surface temperature. At high surface temperatures of about 300 K, F_{net} is less negative and of order -60 Wm^{-2}, despite large surface emission of long-wave irradiance. This is a result of large total column moisture in regions of high T_s which causes atmospheric emission of long-wave irradiance to the surface to be large. In essence, an unstable feedback in the tropics (whereby spatial increases in temperature act to decrease surface clear-sky long-wave radiative cooling) must be counterbalanced by other mechanisms to explain the relatively stable tropical sea surface temperatures (see discussion in Pierrehumbert (1995)).

Over the seasonal cycle, this simulated clear-sky long-wave radiative feedback also applies to much of the globe. $dF_{net}/dT_s > 0\ Wm^{-2}K^{-1}$ for the majority of grid points for July minus January, 1985. Over monthly and interannual time-scales positive dF_{net}/dT_s applies only locally where large perturbations to the atmosphere are apparent. This suggests that changes in large scale atmospheric circulation are required to explain the apparent unstable feedback, rather than local thermodynamic constraints.

Validation of the CLERA simulation is attempted using a simple expression developed by Prata (1996). A spread of about 20 Wm^{-2} in $F_{prata} - F_{net}$ is small considering simulation and observed irradiance accuracy and therefore partially validates simulation monthly means. A systematic $F_{prata} - F_{net}$ positive difference implies overestimation by the formula or underestimation by the simulation or both. A likely cause of underestimation by CLERA is that ECMWF profiles are too

dry (Slingo et al., 1997). One source of potential simulation error is shown, using ECMWF and radiosonde retrievals, to be the surface temperature specification.

Comparison of CLERA with in situ observations over a 6-hourly time-scale is assessed. F_{net} appears too high relative to the observations, although this is likely to be a result of errors in both simulation and observation. High F_{net} variability over a period of a few days occurs in both observation and simulation, which acts to partially validate simulated irradiance. During November 1992, a period of anomalously negative F_{net} is shown to originate over Australia and to propagate northwards. This marked a transition between phases of the Intra Seasonal Oscillation.

Simulated clear-sky surface net long-wave irradiance is shown to be primarily affected by total column moisture. Spatially and over the seasonal cycle changes in T_s result in an apparantly unstable long-wave radiative feedback with surface long-wave cooling decreasing with increasing T_s. Interannual and monthly changes in T_s only reproduce this unstable feedback when changes in the atmospheric structure imply that large scale dynamical changes are significant. This suggests that large scale dynamical changes are required to explain the surface super greenhouse effect (see discussion in Inamdar and Ramanathan (1994)). However, simple thermodynamics are sufficient to explain the increases in total column moisture with surface temperature which act to offset decreases in F_{net} due to increasing surface emission. While the effects of clouds are beyond the scope of this study, results add weight to evidence of a positive water vapour feedback to sea surface temperature. Further validation of simulated surface irradiance with observations is required to add weight to simulated surface irradiance variability over the oceans.

Acknowledgements. The authors thank Dr. Keith Shine for stimulating discussion. Thanks also to Alison Pamment for help in extracting data.

References

Angell, J. K., Variations and trends in tropospheric and stratospheric global temperatures, 1958-1987, *J.Climate Appl.Meteor*, *1*, 1296–1313, 1988.

Dutton, E. G., An extended comparison between LOWTRAN7 computed and observed broadband thermal irradiance: Global extreme and immediate surface conditions, *J.Atmos.Oceanic Techno.*, *10(3)*, 326–336, 1993.

Edwards, J. M. and Slingo, A., Studies with a flexible new radiation code: I: Choosing a configuration for a large scale model, *Quart.J.Roy.Meteorol.Soc.*, *122*, 689–719, 1996.

Gutzler, D. S., Kiladis, G. N., Meehl, G. A., Weickmann, K. M., and Wheeler, M., The global climate of December 1992-February 1993. part II: Large-scale variability across the tropical western pacific during TOGA COARE, *J.Climate*, *7*, 1606–1622, 1994.

Hartmann, D. L. and Michelsen, M. L., Large-scale effects on the regulation of tropical sea surface temperatures, *J.Climate*, *6*, 2049–2062, 1993.

Hess, S. L., *Introduction to Theoretical Meteorology*, Henry Holt and Co., New York, 1959.

Inamdar, A. K. and Ramanathan, V., Physics of greenhouse effect and convection in warm oceans, *J.Climate*, *7*, 715–731, 1994.

IPCC, *Climate Change, the IPCC Scientific Assessment*, Cambridge University Press, 1990.

Long, C. N., Broad-area radiative energy budget, cloud forcing, and column heating rates for the TOGA COARE IFA, Proc. 21st Conf. on Huricanes and Tropical Meteorology, Miami Fla., April 24-28, 1995.

Manabe, S. and Wetherald, R. T., Thermal equilibrium of the atmosphere with a given distribution of relative humidity, *J.Atmos.Sci.*, *24*, 241–259, 1967.

McClatchey, R. A., Fenn, R. A., Selby, R. A., Voltz, P. E., and Garing, J. S., Environmental research paper, Tech. Rep. 411, Air Force Cambridge Research Labs., MA., 1972.

Pierrehumbert, R. T., Thermostats, radiator fins and the local runaway greenhouse effect, *J.Atmos.Sci.*, *52*, 1784–1806, 1995.

Prata, A. J., A new longwave formula for estimating downwelling clear sky radiation at the surface, *Quart.J.Roy.Meteorol.Soc.*, *122*, 1127–1151, 1996.

Reynolds, R. W., A real-time global sea surface temperature analysis, *J.Climate*, *1*, 75–86, 1988.

Rossow, W. B. and Zhang, Y. C., Calculations of surface and top of atmosphere radiative fluxes from physical quantities based on ISCCP data sets. 2. validation and first results, *J.Geophys.Res.*, *100*, 1167–1197, 1995.

Seager, R., Kushnir, Y., and Cane, M. A., On heat flux boundary conditions for ocean models, *J.Phys.Ocean.*, *25*, 3219–3230, 1995.

Shine, K. P., On the cause of the relative greenhouse strength of gases such as the halocarbons, *J.Atmos.Sci.*, *48*, 1513–1518, 1991.

Slingo, A., Pamment, J. A., and Webb, M. J., a 15-year simulation of the clear-sky greenhouse effect using the ECMWF re-analyses: Fluxes and comparisons with ERBE, *J.Climate*, *Submitted*, 1997.

Vonder Haar, T., Surface radiation budget observations and analysis. Position paper in a report of the workshop on surface radiation budget for climate applications., *World Climate Research Program. WCP-115, WMO/TD*, *109*, 144p, 1986.

Webb, M. J., Slingo, A., and Stephens, G. L., Seasonal variations of the clear sky greenhouse effect: the role of changes in atmospheric temperature and humidities, *Climate Dynamics*, *9*, 117–129, 1993.

Weller, R. A. and Anderson, S. P., Surface meteorology and air-sea fluxes in the western equatorial pacific warm pool during the TOGA coupled ocean-atmosphere response experiment, *J.Climate*, *9*, 1959–1990, 1996.

Zhao, W., Khun, W. R., and Drayson, S. R., The significance of detailed structure in the boundary layer to thermal radiation at the surface in climate models, *Geophys.Res.Lett.*, *21*, 1631–1635, 1994.